BIT manuscript No.
(will be inserted by the editor)

Stability Ordinates of Adams Predictor-Corrector Methods

Michelle L. Ghrist · **Bengt Fornberg** · **Jonah A. Reeger**

Received: date / Accepted: date

Abstract How far the stability domain of a numerical method for approximating solutions to differential equations extends along the imaginary axis indicates how useful the method is for approximating solutions to wave equations; this maximum extent is termed the imaginary stability boundary, also known as the stability ordinate. It has previously been shown that exactly half of Adams-Bashforth (AB), Adams-Moulton (AM), and staggered Adams-Bashforth methods have nonzero stability ordinates. In this paper, we consider two categories of Adams predictor-corrector methods and prove that they follow a similar pattern. In particular, if p is the order of the method, ABp-AMp methods have nonzero stability ordinate only for $p = 1,2,\ 5,6,\ 9,10,\ldots$, and AB$(p-1)$-AM$p$ methods have nonzero stability ordinates only for $p = 3,4,\ 7,8,\ 11,12,\ldots$.

Keywords Adams methods · Predictor-corrector · Imaginary stability boundary · Linear multistep methods · Finite difference methods · Stability region · Stability ordinate

Mathematics Subject Classification (2000) 65L06 · 65L12 · 65L20 · 65M06 · 65M12

1 Introduction

When wave equations are posed as first-order systems and discretized in space to yield a system of ordinary differential equations (ODEs), a purely imaginary spectrum will correspond to the fact that only propagation takes place. Many classical numerical methods for

Support for M. Ghrist and J. Reeger provided by the United States Air Force. Support for B. Fornberg provided by NSF DMS-0914647.

Michelle Ghrist
Department of Mathematical Sciences, United States Air Force Academy, USAF Academy, CO 80840, USA
E-mail: michelle.ghrist@usafa.edu

Bengt Fornberg
Department of Applied Mathematics, Campus Box 526, University of Colorado, Boulder, CO 80309, USA
E-mail: fornberg@colorado.edu

Jonah Reeger
Air Force Institute of Technology, 2950 Hobson Way, WPAFB, OH 45433, USA E-mail: jonah.reeger@afit.edu

ODEs have stability regions that include an interval of the form $[-iS_I, iS_I]$ on the imaginary axis. We call the largest such value of S_I the *imaginary stability boundary (ISB)* of the ODE integrator, which is also known as the stability ordinate. In the context of solving semidiscrete wave equations, one desires to use a method with a large ISB, which allows larger stable time steps; methods with zero ISB's (i.e., no imaginary axis coverage in the stability domain) will be unconditionally unstable. In this paper, we explore the question of which Adams methods have nonzero ISB's.

Adams-Bashforth (AB), Adams-Moulton (AM), and Adams predictor-corrector methods are widely used multistep methods for approximating solutions to first-order differential equations. In general, these methods maintain reasonably good accuracy and stability properties and have lower computational costs than equivalent-order Runge–Kutta methods; AB and AM methods require only one new function evaluation per time step, while predictor-corrector methods require two function evaluations [1],[6],[7],[9].

A standard m-step Adams method for approximating solutions to $\frac{dy}{dt} = f(t,y)$ has the form

$$y_{j+1} = y_j + \int_{t_j}^{t_{j+1}} q(t)dt, \tag{1}$$

where $t_j = t_0 + jh$, h is the stepsize, and $y_0 = y(t_0)$. Here, $q(t)$ is the polynomial interpolating the points (t_k, y_k) for $j-m+1 \le k \le j$ (AB methods) or $j-m+1 \le k \le j+1$ (AM methods). We will henceforth use $j = 0$ to simplify the notation. AB methods have order $p = m$ while AM methods have order $p = m+1$.

For staggered AB methods, $q(t)$ in (1) interpolates at $\left(t_{k+1/2}, y_{k+1/2}\right)$ for $j-m+1 \le k \le j$; like AB methods, these methods have order $p = m$. For a given order of accuracy, staggered multistep methods have about ten times less local truncation error and stability domains that extend approximately 2-8 times as far on the imaginary axis when compared to their nonstaggered counterparts [4]. This improved accuracy and stability with no additional computational or storage cost makes such methods ideal when they can be applied; their main use is in approximating solutions to linear wave equations, which can be formulated with a grid which is staggered in space and/or time. For broader studies of staggered methods (to include more general multistep and Runge–Kutta methods), see [4], [5].

In [2, Table G.3-1], it was observed (without proof) that AB methods of order p (ABp) have nonzero ISB's only for orders $p = 3,4,\ 7,8,\ 11,12,\ldots$ and AMp methods have nonzero ISB's only for orders $p = 1,2,\ 5,6,\ 9,10,\ldots$. These results can be deduced from [10] and were independently shown in [3] and [4]. While [10] is not applicable to staggered methods, [3] and [4] proved that staggered AB methods of order p have nonzero ISB's only for $p = 2,3,4,\ 7,8,\ 11,12,\ldots,$; none of the aforementioned articles addressed Adams predictor-corrector methods. Henceforth, we will only consider nonstaggered methods.

This study revisits our previous results from [4] with a new formulation and then extends our results to Adams predictor-corrector methods. In particular, we examine the most commonly used Adams predictor-corrector methods ABp-AMp and AB($p-1$)-AMp, both of which have order p. We are unaware of any other studies addressing the ISB's of such methods for general order p. In [2, Table G.3-1], it was claimed that for such methods, 'most' had nonzero ISB's while 'some' had zero ISB's. We now proceed with proving that such methods follow very similar patterns to those of AB and AM methods, with ABp-AMp methods following the same pattern as AMp methods and AB($p-1$)-AMp methods following the same pattern as ABp methods. We then offer an application illustrating the significance of these results.

2 Preliminary Results

When solving Dahlquist's linear test problem

$$\frac{dy}{dt} = \lambda y, \tag{2}$$

the edge of a stability domain is described by the root $\xi = \lambda h$ of $\rho(r) - \xi\sigma(r) = 0$ when r travels around the unit circle $r = e^{i\theta}$. Here, $\rho(r)$ and $\sigma(r)$ are the generating polynomials of the method (see, e.g., [9, p. 27]).

To consider whether or not a stability domain has imaginary axis coverage, we wish to describe the behavior of the stability domain boundary near $\xi = 0$. For an exact method, we have $\xi(\theta) = \ln r$ (see, e.g., [9, Theorem 2.1], using $\xi = \frac{\rho(r)}{\sigma(r)}$.) Thus the stability boundary of an exact method satisfies

$$\xi = \ln r = \ln\left(e^{i\theta}\right) = i\theta \tag{3}$$

near $\xi = 0$. A numerical scheme of order p will instead lead to

$$\xi(\theta) = i\theta + c_p(i\theta)^{p+1} + d_p(i\theta)^{p+2} + O\left((i\theta)^{p+3}\right) \tag{4}$$

for some constants c_p and d_p. The sign of the first *real* term in the expansion (4) will dictate whether the stability domain boundary near the origin swings to the right or to the left of the imaginary axis.

For example, AB2 has the expansion $\xi(\theta) = i\theta + \frac{5}{12}(i\theta)^3 - \frac{1}{4}(i\theta)^4 + \ldots$; because the sign of the first real term in this expansion is negative, the ISB of AB2 is zero. AB3 has the expansion $\xi(\theta) = i\theta + \frac{3}{8}(i\theta)^4 + \ldots$; because the sign of the first real term in this expansion is positive, the ISB of AB2 is positive. See Figure 1 for an illustration comparing the stability domains of AB2 (which has a zero ISB) and AB3 (which has an ISB of $\frac{12}{5\sqrt{11}} \approx 0.724$.)

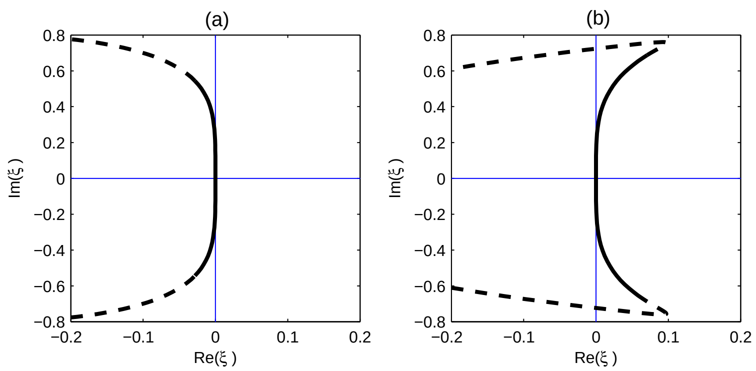

Fig. 1 Shown are portions of the boundaries of the stability regions for (a) AB2 and (b) AB3. The solid line marks the presently relevant section of the stability domain boundary near the origin; the stability regions consist of the regions to the left of the boundary. Both graphs show that $\xi \approx i\theta$ near $\xi = 0$. When the first real term in (4) is negative, the ISB is 0. (b) When the first real term in (4) is positive, the ISB is nonzero. The intercepts of AB2 and AB3 on the negative real axis are -1 and $-\frac{6}{11}$, respectively.

2.1 Backward difference forms of AB and AM methods

In [8, pp. 191-195], Henrici gave a backward difference representation of (1) for AB and AM methods. When applied to (2), an m-step AB method can be represented by

$$y_1 = y_0 + h\lambda \sum_{k=0}^{m-1} \gamma_k \nabla^k y_0, \tag{5}$$

where

$$\gamma_k = (-1)^k \int_0^1 \binom{-s}{k} ds. \tag{6}$$

Similarly, an m-step AM method can be represented by

$$y_1 = y_0 + h\lambda \sum_{k=0}^{m} \gamma_k^* \nabla^k y_1, \tag{7}$$

where

$$\gamma_k^* = (-1)^k \int_0^1 \binom{-s+1}{k} ds. \tag{8}$$

Henrici [8, p. 195] also established that

$$\sum_{j=0}^{k} \gamma_j^* = \gamma_k, \tag{9}$$

from which

$$\gamma_k^* = \gamma_k - \gamma_{k-1}. \tag{10}$$

Lemma 2.1 *For all integers $k \geq 1$, $\gamma_k^* < 0$. For all integers $k \geq 0$, $\gamma_k > 0$. For all integers $k \geq 3$, $\gamma_k > \frac{1}{k}$.*

Proof Evaluating (8) directly gives $\gamma_0^* = 1$ and $\gamma_1^* = -\frac{1}{2}$. For the general case when $k \geq 1$, we rewrite (8) to find

$$\gamma_k^* = \frac{1}{k!} \int_0^1 (s-1)s(s+1)(s+2)\dots(s+k-2)ds. \tag{11}$$

The integrand is negative for $0 < s < 1$, so $\gamma_k^* < 0$ for $k \geq 1$.

We next note that an alternate way to express (6) is

$$\gamma_k = \frac{1}{k!} \int_0^1 s(s+1)(s+2)\dots(s+k-1)\, ds. \tag{12}$$

Direct evaluation of (12) gives $\gamma_0 = 1$, $\gamma_1 = \frac{1}{2}$, $\gamma_2 = \frac{5}{12}$, and $\gamma_3 = \frac{3}{8} > \frac{1}{3}$. We now prove the last part of the lemma via induction. We assume that $\gamma_j > \frac{1}{j}$ for some $j \geq 3$ and seek to establish that $\gamma_{j+1} > \frac{1}{j+1}$. From (12),

$$\gamma_{j+1} = \int_0^1 \frac{s(s+1)(s+2)\dots(s+j-1)}{j!} \left(\frac{s+j}{j+1}\right) ds > \left(\frac{j}{j+1}\right)\gamma_j > \left(\frac{j}{j+1}\right)\frac{1}{j} = \frac{1}{j+1}.$$

Thus $\gamma_k > \frac{1}{k}$ by induction for all integers $k \geq 3$, and $\gamma_k > 0$ for all integers $k \geq 0$. □

Table 1 gives the first six values of γ_k and γ_k^*.

m	0	1	2	3	4	5
γ_m	1	$\frac{1}{2}$	$\frac{5}{12}$	$\frac{3}{8}$	$\frac{251}{720}$	$\frac{95}{288}$
γ_m^*	1	$-\frac{1}{2}$	$-\frac{1}{12}$	$-\frac{1}{24}$	$-\frac{19}{720}$	$-\frac{3}{160}$

Table 1 First six values of γ_k and γ_k^* from (12) and (11). These results match Tables 5.2 and 5.4 of [8].

2.2 Exact solution

Using $\xi = \lambda h$, the exact solution to (2) is $y(t) = e^{\lambda t} = e^{\xi t/h}$ where, without loss of generality, we have chosen $t_0 = 0$ and $y(t_0) = 1$. For an exact method, $\xi = i\theta$ near $\xi = 0$ from (3), so

$$y_n = y(nh) = e^{in\theta}. \tag{13}$$

An alternate way to view (13) is that we are seeking the exact solution to the relevant difference equation when following the root r that has $r = e^{i\theta}$, which gives $y_n = r^n = \left(e^{i\theta}\right)^n = e^{in\theta}$.

We now give a lemma that will help in finding the expansion (4) for general order Adams methods.

Lemma 2.2 *For integers $k \geq 1$, when $y_n = e^{in\theta}$*

$$\nabla^k y_0 = (i\theta)^k \left[1 - \frac{k}{2}(i\theta) + O\left((i\theta)^2\right)\right], \tag{14}$$

and

$$\nabla^k y_1 = (i\theta)^k \left[1 + \frac{2-k}{2}(i\theta) + O\left((i\theta)^2\right)\right]. \tag{15}$$

For integers $M \geq 1$, when $y_n = e^{in\theta}$,

$$\sum_{k=0}^{M} \gamma_k \nabla^k y_0 = 1 + \frac{1}{2}(i\theta) + O\left((i\theta)^2\right) \tag{16}$$

and

$$\sum_{k=0}^{M} \gamma_k^* \nabla^k y_1 = 1 + \frac{1}{2}(i\theta) + O\left((i\theta)^2\right). \tag{17}$$

Proof For $y_n = e^{in\theta}$, $\nabla y_0 = \left(1 - e^{-i\theta}\right)$ and $\nabla^k y_0 = \left(1 - e^{-i\theta}\right)^k$ so that

$$\begin{aligned}
\nabla^k y_0 &= \left[1 - \left(1 + (-i\theta) + \frac{1}{2!}(-i\theta)^2 + O\left((i\theta)^3\right)\right)\right]^k \\
&= (i\theta)^k \left[1 - \frac{k}{2}(i\theta) + O\left((i\theta)^2\right)\right],
\end{aligned}$$

establishing (14). For $y_n = e^{in\theta}$, $\nabla^k y_1 = e^{i\theta}\nabla^k y_0$. Multiplying (14) by $e^{i\theta} = 1 + i\theta + \ldots$ gives (15).

Using (14), we find

$$\begin{aligned}\sum_{k=0}^{M} \gamma_k \nabla^k y_0 &= \sum_{k=0}^{M} \gamma_k (i\theta)^k \left[1 - \frac{k}{2}(i\theta) + O\left((i\theta)^2\right)\right] \\ &= \gamma_0 \left[1 + O\left((i\theta)^2\right)\right] + \gamma_1 (i\theta)\left[1 + O(i\theta)\right] + O\left((i\theta)^2\right) \\ &= 1 + \frac{1}{2} i\theta + O\left((i\theta)^2\right),\end{aligned}$$

where we have used $\gamma_0 = 1$ and $\gamma_1 = \frac{1}{2}$ in the last step. This establishes (16). A similar expansion using (15), $\gamma_0^* = 1$, and $\gamma_1^* = -\frac{1}{2}$ gives (17). □

In the next section, we apply these results to obtain the expansion (4) for general ABp and AMp methods. In Section 4, we apply these results to obtain the expansion (4) for general ABp-AMp methods and AB($p-1$)-AMp methods.

3 Revisiting stability ordinates for AB and AM methods

We now apply the backward difference forms of the Adams methods to consider the ISB's of general AB and AM methods, thereby giving an alternate proof to [4].

Theorem 3.1 *AB methods have nonzero ISB's only for orders* $p = 3, 4,\ 7, 8,\ \ldots$.

Proof We first note that it is well known that the ISB for AB1 (Euler's method) is zero (see, for example [2]). One can also check the expansion; AB1 has an expansion of $\xi = e^{i\theta} - 1 = i\theta + \frac{1}{2}(i\theta)^2 + \ldots$, which has a negative first real term, confirming that the ISB for AB1 is zero. We now proceed with the general case for $p \geq 2$.

For AB methods, we will show that $c_p > 0$ and $d_p < 0$ for all orders $p \geq 2$, where c_p and d_p are defined by (4). The pattern for which methods have nonzero ISB's then follows from the powers of the imaginary unit in (4). For example, for $p = 3$, the first real term in the expansion (4) is $c_3(i\theta)^4 = c_3\theta^4 > 0$. Thus the boundary of the stability domain of AB3 swings to the right of the imaginary axis near the origin, and we have a nonzero ISB for this method, as seen in Figure 1b. For $p = 6$, the first real term in the expansion (4) is $d_6(i\theta)^8 = d_6(\theta)^8 < 0$; thus the stability domain boundary of AB6 swings to the left of the imaginary axis near the origin, and the ISB of this method is zero.

We seek to find the values of c_p and d_p in the case of a general ABp method. We apply (13) to (5), using $\xi = \lambda h$ to find

$$e^{i\theta} = 1 + \xi \sum_{k=0}^{m-1} \gamma_k \nabla^k y_0. \tag{18}$$

As $m \to \infty$, the AB method (5) reproduces the exact solution. Thus, using (3), we find

$$e^{i\theta} = 1 + i\theta \sum_{k=0}^{\infty} \gamma_k \nabla^k y_0. \tag{19}$$

Combining (19) and (18) gives

$$(\xi - i\theta) \sum_{k=0}^{m-1} \gamma_k \nabla^k y_0 = i\theta \sum_{k \geq m} \gamma_k \nabla^k y_0.$$

We now substitute for ξ using (4), where the order $p = m$ for AB. Using (14) and (16), we find

$$\left[c_m (i\theta)^{m+1} + d_m (i\theta)^{m+2} + O\left((i\theta)^{m+3}\right)\right]\left[1 + \frac{1}{2}(i\theta) + O\left((i\theta)^2\right)\right]$$
$$= \gamma_m (i\theta)^{m+1}\left[1 - \frac{m}{2}(i\theta) + O\left((i\theta)^2\right)\right] + \gamma_{m+1}(i\theta)^{m+2}\left[1 + O(i\theta)\right] + O\left((i\theta)^{m+3}\right).$$

Collecting like powers of $i\theta$, we find that $c_m = \gamma_m$ and

$$\frac{1}{2}c_m + d_m = \gamma_m\left(-\frac{m}{2}\right) + \gamma_{m+1}$$

so that

$$d_m = \gamma_{m+1} - \frac{m}{2}\gamma_m - \frac{1}{2}c_m = \gamma_{m+1} - \left(\frac{m+1}{2}\right)\gamma_m. \tag{20}$$

From Lemma 2.1, we have $c_m = \gamma_m > 0$ for integers $m \geq 0$. Using this result and (12) in (20) gives

$$\begin{aligned} d_m &= \gamma_{m+1} - \left(\frac{m+1}{2}\right)\gamma_m \\ &= \frac{1}{2(m+1)!}\int_0^1 s(s+1)(s+2)\cdots(s+m-1)\left[2(s+m)-(m+1)^2\right]ds \\ &= -\frac{1}{2(m+1)!}\int_0^1 s(s+1)(s+2)\cdots(s+m-1)\left[m^2+1-2s\right]ds. \end{aligned}$$

Because $m^2+1-2s > 0$ for $m \geq 2$ and $0 \leq s \leq 1$, the integrand is positive so that $d_m < 0$ for $m \geq 2$. Noting that $p = m$ for AB methods, examining the sign of the first real term in (4) establishes our result that AB methods have nonzero ISB's only for orders $p = 3,4,\ 7,8,\ 11,12,\ldots$. □

Theorem 3.2 *AM methods have nonzero ISB's only for orders* $p = 1,2,\ 5,6,\ 9,10,\ldots$.

Proof We first note that $p = 1$ (Backward Euler) and $p = 2$ (AM2) are well-known A-stable methods and thus have nonzero ISB's; one can also check their expansions. AM1 has an expansion of $\xi = 1 - e^{-i\theta} = i\theta - \frac{1}{2}(i\theta)^2 + \ldots$, which has a positive first real term, indicating that AM1 has a nonzero ISB. The expansion for AM2 contains only purely imaginary terms; this is to be expected since the stability domain boundary for AM2 consists of the entire imaginary axis.

We now prove the general result for $p \geq 3$. We seek to find the values of c_p and d_p in (4) for a general AMp method. We apply (13) to (7), using $\xi = \lambda h$ to find

$$e^{i\theta} = 1 + \xi\sum_{k=0}^{m}\gamma_k^*\nabla^k y_1. \tag{21}$$

As $m \to \infty$, the AM method (7) reproduces the exact solution. Thus, using (3), we find

$$e^{i\theta} = 1 + i\theta\sum_{k=0}^{\infty}\gamma_k^*\nabla^k y_1. \tag{22}$$

Combining (22) and (21) gives

$$(\xi - i\theta)\sum_{k=0}^{m}\gamma_k^*\nabla^k y_1 = i\theta\sum_{k\geq m+1}\gamma_k^*\nabla^k y_1.$$

We now substitute for ξ using (4), where the order $p = m+1$ for AM. Using (15) and (17), we find

$$\left[c_m (i\theta)^{m+2} + d_m (i\theta)^{m+3} + O\left((i\theta)^{m+4}\right)\right]\left[1 + \frac{1}{2}(i\theta) + O\left((i\theta)^2\right)\right]$$
$$= \gamma^*_{m+1} (i\theta)^{m+2}\left[1 + \frac{1-m}{2}(i\theta) + O\left((i\theta)^2\right)\right] + \gamma^*_{m+2} (i\theta)^{m+3}\left[1 + O(i\theta)\right] + O\left((i\theta)^{m+4}\right).$$

Collecting like powers of $i\theta$, we find that $c_m = \gamma^*_{m+1}$ and

$$\frac{1}{2}c_m + d_m = \gamma^*_{m+2} - \gamma^*_{m+1}\left(\frac{m-1}{2}\right). \tag{23}$$

From Lemma 2.1, we have $c_m = \gamma^*_{m+1} < 0$ for $m \geq 1$. Using this result and (11) in (23) and simplifying gives

$$\begin{aligned} d_m &= \gamma^*_{m+2} - \left(\frac{m}{2}\right)\gamma^*_{m+1} \qquad (24)\\ &= \frac{1}{2(m+2)!}\int_0^1 (s-1)s(s+1)(s+2)\cdots(s+m-1)\left(2s-m^2\right)ds. \end{aligned}$$

Because $(s-1)$ and $(2s-m^2)$ are both negative for $0 < s < 1$ and $m \geq 2$, the integrand is positive for $m \geq 2$. Therefore $d_m > 0$ and $c_m < 0$ for AM methods, exactly opposite the result for AB methods. After examining the sign of the first real term in (4) and noting that $p = m+1$ for AM methods, we conclude that Adams-Moulton methods have nonzero ISB's only for orders $p = 1, 2,\ 5, 6,\ 9, 10, \ldots$. □

4 Stability ordinates of Adams predictor-corrector methods

We now examine two different categories of Adams predictor-corrector methods: ABp-AMp methods and AB($p-1$)-AMp methods.

4.1 Two examples

We first consider two examples, AB1-AM2 and AB2-AM2. The predictor AB1 is given by

$$y_1^P = y_0 + hf(t_0, y_0), \tag{25}$$

and the predictor AB2 is given by

$$y_1^P = y_0 + \frac{h}{2}\left(3f(t_0, y_0) - f(t_{-1}, y_{-1})\right). \tag{26}$$

In both cases, the corrector AM2 is given by

$$y_1 = y_0 + \frac{h}{2}\left(f\left(t_1, y_1^P\right) + f(t_0, y_0)\right). \tag{27}$$

We first consider AB1-AM2. Using (25), substituting $f(t,y) = \lambda y = \frac{\xi}{h}y$, and letting $y_k = r^k$ to solve the resulting difference equation, we find that (27) becomes

$$r = 1 + \frac{1}{2}\xi(1+\xi) + \frac{1}{2}\xi. \tag{28}$$

To find the boundary of the stability domain, we follow the root ξ in (28) near $\xi = 0$ where $|r| = 1$. The stability domain of this method is shown in Figure 2(a). We can also let $r = e^{i\theta}$ and do a Taylor expansion for $\xi(\theta)$ in (28) to find that

$$\xi = i\theta + \frac{1}{6}(i\theta)^3 - \frac{1}{8}(i\theta)^4 + \dots. \tag{29}$$

Because the first real term in this expansion is negative, AB1-AM2 has a zero ISB.

We next consider AB2-AM2. Using (26) and (27), we find that the analogous equation to (28) is

$$r^2 = r + \frac{1}{2}\xi\left(r + \frac{\xi}{2}(3r-1)\right) + \frac{1}{2}\xi r,$$

which leads to the expansion

$$\xi = i\theta - \frac{1}{12}(i\theta)^3 + \frac{1}{4}(i\theta)^4 + \dots. \tag{30}$$

Since the first real term in this expansion is positive, AB2-AM2 has a nonzero ISB (approximately 1.29). The stability domain of this method is shown in Figure 2(b).

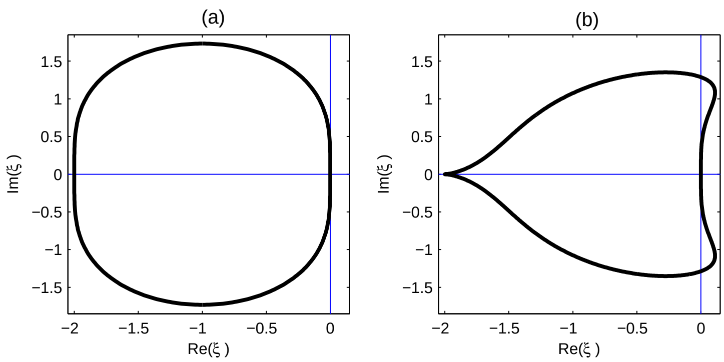

Fig. 2 Shown are the boundaries of the stability regions for (a) AB1-AM2 and (b) AB2-AM2. The stability regions consist of the inside of these curves. For (b), the ISB is approximately 1.29. The intercept on the negative real axis is -2 for both methods.

4.2 General order predictor-corrector methods

In general, from (5), our AB predictor will take the form

$$y_1^P = y_0 + \xi \sum_{k=0}^{M} \gamma_k \nabla^k y_0 \tag{31}$$

where $M = m-1$ for AB($p-1$)-AMp methods and $M = m$ for ABp-AMp methods; both methods have order $p = m+1$. The general form of the AM corrector method is given by

(7), where we replace all instances of y_1 on the right-hand side by y_1^P after the backward difference operations are done. This leads to

$$\begin{aligned} y_1 &= y_0 + \xi \sum_{j=0}^{m} \gamma_k^* \nabla^k y_1 + \xi \left(\gamma_0^* + \gamma_1^* + \cdots \gamma_m^*\right) \left(y_1^P - y_1\right) \\ &= y_0 + \xi \sum_{j=0}^{m} \gamma_k^* \nabla^k y_1 + \xi \gamma_m \left(y_1^P - y_1\right), \end{aligned} \tag{32}$$

where we have used (9) in the last step.

We use (31) to substitute for y_1^P in (32) and then use the exact solution (13) to find

$$e^{i\theta} = 1 + \xi \sum_{j=0}^{m} \gamma_k^* \nabla^k y_1 + \xi \gamma_m \left(1 - e^{i\theta} + \xi \sum_{k=0}^{M} \gamma_k \nabla^k y_0\right). \tag{33}$$

We now use the exact AM and AB expressions (22) and (19) to substitute for the two instances of $e^{i\theta}$ in (33) respectively. Simplifying gives

$$\begin{aligned} 0 = (\xi - i\theta)&\left(\sum_{k=0}^{m} \gamma_k^* \nabla^k y_1\right) - i\theta \sum_{k\geq m+1} \gamma_k^* \nabla^k y_1 \\ &+ \xi \gamma_m \left[(\xi - i\theta)\left(\sum_{k=0}^{M} \gamma_k \nabla^k y_0\right) - i\theta \sum_{k\geq M+1} \gamma_k \nabla^k y_0\right], \end{aligned}$$

where $M = m-1$ for AB($p-1$)-AMp methods and $M = m$ for ABp-AMp methods.

Applying Lemma 2.2 gives

$$\begin{aligned} 0 = (\xi - i\theta)&\left(1 + \frac{i\theta}{2} + O\left((i\theta)^2\right)\right) - i\theta \sum_{k\geq m+1} \gamma_k^* \left[(i\theta)^k \left(1 + \frac{2-k}{2}(i\theta) + \cdots\right)\right] \\ &+ \xi \gamma_m \left[(\xi - i\theta)(1 + O(i\theta)) - i\theta \sum_{k\geq M+1} \gamma_k (i\theta)^k \left(1 - \frac{k}{2}(i\theta) + O\left((i\theta)^2\right)\right)\right]. \end{aligned} \tag{34}$$

This formula permits us to compute the expansion of the boundary of the stability region $\xi(\theta)$ near the origin for the two Adams predictor-corrector methods of present interest. We first consider general ABp-AMp methods, which have order p.

Theorem 4.1 *Predictor-corrector ABp-AMp methods have nonzero ISB's only for orders $p = 1,2,\ 5,6,\ 9,10,\ldots$.*

Proof Our general proof will require $p \geq 3$. For $p = 1$, we can find that the series expansion for the combination of forward Euler predictor and backward Euler correction is $\xi = i\theta - \frac{1}{2}(i\theta)^2 + \cdots$. Because this has a positive first real term, AB1-AM1 also has a nonzero ISB. For $p = 2$, we have already established that AB2-AM2 has a nonzero ISB via (30); also see Figure 2(b).

We let $M = m$ in (34) and substitute (4), using $p = m+1$ to find

$$\begin{aligned} 0 = &\left(c_m (i\theta)^{m+2} + d_m (i\theta)^{m+3} + \cdots\right)\left(1 + \frac{i\theta}{2} + \gamma_m (i\theta + \cdots)\right) \\ &- i\theta \sum_{k\geq m+1} \gamma_k^* (i\theta)^k \left(1 - \frac{k-2}{2}(i\theta) + \cdots\right) \\ &- (i\theta)^2 \gamma_m \sum_{k\geq m+1} \gamma_k (i\theta)^k \left(1 - \frac{k}{2}(i\theta) + \cdots\right) + \cdots, \end{aligned} \tag{35}$$

where we have kept only the terms that are needed to find the dominant terms in this expression. Examining the coefficients of the $(i\theta)^{m+2}$ and $(i\theta)^{m+3}$ terms in (35) gives:

$$c_m = \gamma^*_{m+1} \tag{36}$$

and

$$d_m = \gamma^*_{m+2} - \gamma^*_{m+1}\frac{m-1}{2} + \gamma_m\gamma_{m+1} - c_m\left(\frac{1}{2}+\gamma_m\right). \tag{37}$$

From Lemma (2.1), we know that $c_m < 0$ for $m \geq 1$. Simplifying (37) using (36) and (10) gives

$$d_m = \gamma^*_{m+2} - \frac{m}{2}\gamma^*_{m+1} + \gamma_m^2.$$

From (24), we know that $\gamma^*_{m+2} - \frac{m}{2}\gamma^*_{m+1} > 0$ for $m \geq 2$, so we have $d_m > 0$ for $m \geq 2$. Thus $c_m < 0$ and $d_m > 0$ for $m \geq 2$ where $p = m+1$. After examining the sign of the first real term in (4) for this case, we conclude that ABp-AMp methods have nonzero ISB's only for orders $p = 1,2,\ 5,6,\ 9,10,\ldots$, a result identical to AMp methods. $\square$

Figure 3 shows the stability domains of AB$(p-1)$-AMp and ABp-AMp methods near the origin.

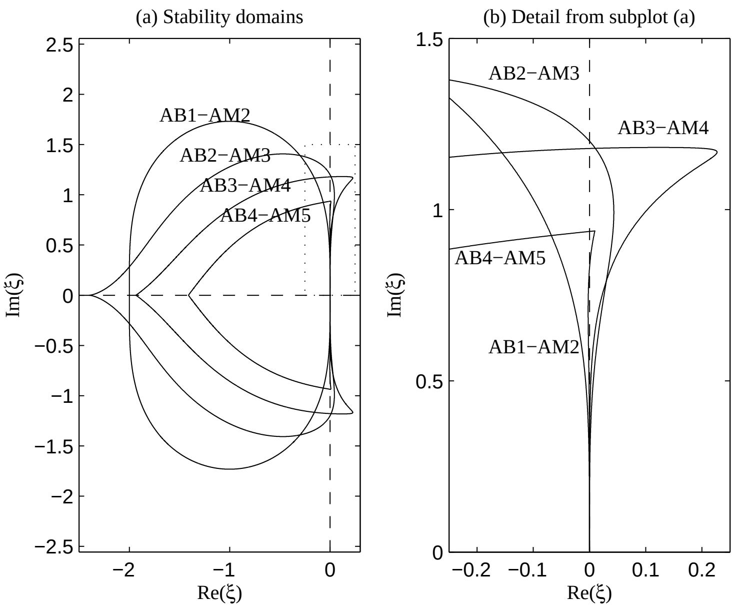

Fig. 3 (a) Shown are the relevant portions of the boundaries of the stability regions for AB$(p-1)$-AMp methods; the stability domain consists of the interior of each curve. (b) The detail splot shows that AB2-AM3 and AB3-AM4 are the only methods shown with nonzero ISB. While the stability domain for AB4-AM5 does include part of the first quadrant, the boundary initially swings into the second quadrant, reflecting a zero ISB.

We now examine general AB$(p-1)$-AMp methods, which also have order $p = m+1$.

Theorem 4.2 *Predictor-corrector AB($p-1$)-AMp methods have nonzero ISB's only for orders $p = 3,4,\ 7,8,\ldots$.*

Proof Our general proof will require $p \geq 3$. For $p = 2$, we have already established that AB1-AM2 has a zero ISB via (29); also see Figure 2(a).

We now proceed with the general case for $p \geq 3$. We let $M = m-1$ in (34) and substitute (4), using $p = m+1$ to find

$$\begin{aligned} 0 = &\left(c_m\,(i\theta)^{m+2} + d_m\,(i\theta)^{m+3} + \cdots\right)\left(1 + \frac{i\theta}{2} + \gamma_m\,(i\theta + \cdots)\right) \\ &- i\theta \sum_{k\geq m+1} \gamma_k^*\,(i\theta)^k \left(1 - \frac{k-2}{2}\,(i\theta) + \cdots\right) \\ &- (i\theta)^2\,\gamma_m \sum_{k\geq m} \gamma_k\,(i\theta)^k \left(1 - \frac{k}{2}\,(i\theta) + \cdots\right) + \cdots, \end{aligned} \tag{38}$$

where we have kept only the terms that are needed to find the dominant terms in this expression. Examining the coefficients of the $(i\theta)^{m+2}$ and $(i\theta)^{m+3}$ terms in (38) gives

$$c_m = \gamma_{m+1}^* + \gamma_m^2 \tag{39}$$

and

$$d_m = \gamma_{m+2}^* - \left(\frac{m-1}{2}\right)\gamma_{m+1}^* + \gamma_m\left(\gamma_{m+1} - \frac{m}{2}\gamma_m\right) - c_m\left(\frac{1}{2} + \gamma_m\right). \tag{40}$$

We claim that $c_m < 0$ and $d_m > 0$ for $m \geq 2$. From (39), (40), and Table 1, we compute $c_2 = \frac{329}{2880}$ and $d_2 = -\frac{265}{1536}$. From Lemma 2.1, we have $\gamma_m > \frac{1}{m}$ for $m \geq 3$. Applying this, (12), and (11) to (39) and simplifying gives

$$c_m > \gamma_{m+1}^* + \frac{1}{m}\gamma_m = \frac{1}{m(m+1)!}\int_0^1 (ms+1)s(s+1)(s+2)\ldots(s+m-1)ds > 0$$

for $m \geq 3$ because the integrand is positive.

We now consider the expression for d_m in (40). We substitute for c_m from (39), apply (9) and results from Lemma 2.1, and simplify to find

$$\begin{aligned} d_m &= \gamma_{m+2}^* - \frac{m}{2}\gamma_{m+1}^* + \left(\frac{1-m}{2}\right)\gamma_m^2 - \gamma_m^3 \\ &< \gamma_{m+2}^* - \frac{m}{2}\gamma_{m+1}^* + \left(\frac{1-m}{2}\right)\frac{\gamma_m}{m} \\ &= \frac{1}{2m(m+2)!}\int_0^1 s(s+1)\ldots(s+m-1)\left[\left(2+m-2m^2\right) + ms\left(2s-m^2-2\right)\right] ds \end{aligned}$$

for $m \geq 3$, where we have used (12) and (11) in the last step. Bacause $\left(2+m-2m^2\right)$ and $\left(2s-m^2-2\right)$ are both negative for $0 < s < 1$ and $m \geq 3$, the integrand is negative and thus $d_m < 0$ for $m \geq 3$ for ABp-AMp methods. Thus $c_m > 0$ and $d_m < 0$ for $m \geq 3$ where $p = m+1$. After examining the sign of the first real term in (4), we conclude that AB($p-1$)-AMp methods have nonzero ISB's only for orders $p = 3,4,\ \ 7,8,\ldots$, a result identical to ABp methods. □

Figure 4 show the stability domains of AB($p-1$)-AMp and ABp-AMp methods near the origin. Our results are summarized along with other relevant results from [4] in Table 2. In Section 5, we present a test that both confirms our results and shows the practical significance of our results when solving wave equations.

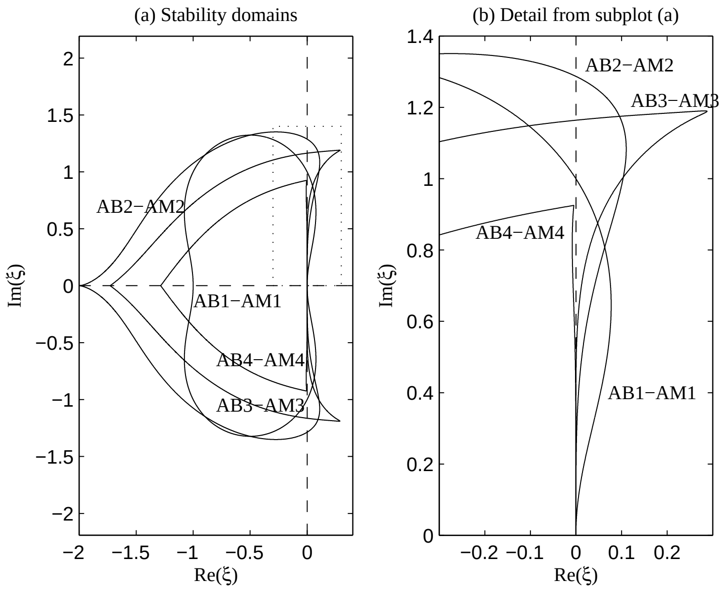

Fig. 4 (a) Shown are relevant portions of the boundaries of the stability regions for ABp-AMp methods; the stability domain consists of the interior of each curve. (b) AB1-AM1 and AB2-AM2 are the only methods shown which have nonzero ISB. While the stability domain for AB3-AM3 does include part of the first quadrant, the boundary initially swings into the second quadrant, reflecting a zero ISB; the enlarged figure (b) does not have enough resolution to see this but further enlargements do.

Method	Orders	Formula (where $k \in \mathbb{Z}^+$)
AB	$3,4,\ 7,8,\ldots$	$\{4k-1,4k\}$
AM	$1,2,\ 5,6,\ldots$	$\{4k-3,4k-2\}$
Staggered AB	$2,3,4,\ 7,8,\ldots$	$\{2\}\bigcup\{4k-1,4k\}$
ABp-AMp	$1,2,\ 5,6,\ldots$	$\{4k-2,4k-1\}$
AB($p-1$)-AMp	$3,4,\ 7,8,\ldots$	$\{4k-1,4k\}$

Table 2 Summary of results of orders for which various methods have nonzero stability ordinates

5 Illustration via application to the 1D wave equation

In this section, we perform analysis that both confirms our results and shows their practical significance when solving wave equations.

Dahlquist's equivalence theorem [9, pp. 24-25] tells that a multistep method is convergent if and only if the method is of order $p \geq 1$ and the generating polynomial $\rho(r)$ of the method obeys the root condition, that is if all roots of $\rho(r)$ satisfy $|r| \leq 1$ and all roots with $|r| = 1$ are simple. For a fixed number of ODEs, this assures that numerical solutions will converge to analytic solutions as the time step Δt approaches 0; this is true for all of the relevant methods that we have considered: ABp, AMp, ABp-AMp, and AB($p-1$)-AMp.

Consider next the one-dimensional wave equation

$$u_t + u_x = 0, \tag{41}$$

which has a purely imaginary spectrum. If we advance (41) on the periodic interval $-\pi \leq x \leq \pi$ from $t = 0$ to $t = 10\pi$, the analytic solution $u(x,t) = u(x-t,0)$ completes five full periods. As is typical when time-stepping a wave equation, we let the mesh aspect ratio $\frac{\Delta t}{\Delta x}$ stay constant as we refine in both x and t.

Let N be the number of equispaced node points in the x-direction. The key difference between solving (41) and solving an ODE (or a system of ODEs) is that, when we refine in the t-direction with the ratio $\frac{\Delta t}{\Delta x}$ held fixed, the number of ODEs N will simultaneously increase, making the root condition no longer applicable for establishing convergence. Thus, we will consider an alternative analysis which is designed to illustrate the convergence properties of the methods of present interest.

An arbitrary initial condition $u(x,0)$ can be decomposed into Fourier modes $e^{i\omega x}$, with $-\frac{\pi}{\Delta x} \leq \omega \leq \frac{\pi}{\Delta x}$. When N is increased, more and more Fourier modes can be represented in the x-direction. Analytically, each mode should remain of unchanged amplitude as time increases; instability presents itself when there is no upper bound on how large a mode can become even after a finite time. Let $R(\omega, N, \frac{\Delta t}{\Delta x})$ be the ratio of the amplitude of a given mode of frequency ω at time $t = 10\pi$ to its amplitude at $t = 0$.

Figure 5 shows $\max_\omega R(\omega, N, \frac{\Delta t}{\Delta x})$, i.e., the amplitude change factor for the fastest growing mode out of all present Fourier modes for the first six AB($p-1$)-AMp methods, which was implemented in MATLAB. Ideally, the surfaces should be perfectly flat at value 0 (as this is a log-log graph), reflecting no growth. We see this to be the case for AB2-AM3, AB3-AM4, and AB6-AM7 whenever the ratio $\frac{\Delta t}{\Delta x}$ is below certain constants, as expected. However, no non-zero value for the ratio $\frac{\Delta t}{\Delta x}$ can salvage AB1-AM2, AB4-AM5, or AB5-AM6 from disastrous spurious growth in the solution under refinement. The surfaces are truncated at the level $\max R = 10^{16}$; this level was chosen because even modes that are theoretically absent (but are actually present at a level of $O(10^{-16})$ due to machine precision) will then have grown to size $O(1)$.

Further simulations show similar behavior for the first six ABp-AMp methods: convergence for AB1-AM1, AB2-AM2, AB5-AM5, and AB6-AM6 whenever the ratio $\frac{\Delta t}{\Delta x}$ is below certain constants, and disastrous growth for AB3-AM3 and AB4-AM4 for all values of the ratio $\frac{\Delta t}{\Delta x}$, thus confirming our observations in Figure 4.

6 Conclusions

We have considered the question of when Adams methods of general order p have nonzero stability ordinates (ISB's). By applying the backward difference formulation of the AB and AM methods [8], we have proven that ABp-AMp methods have nonzero stability ordinates only for $p = 1,2,\ 5,6,\ 9,10,\ldots$, which matches AM$p$ methods. We have also shown that AB($p-1$)-AMp methods have nonzero stability ordinates only for $p = 3,4,\ 7,8,\ 11,12,\ldots$, which matches AB$p$ methods. Discovering intuitive heuristic motivations for these patterns remains an open challenge. While a method having nonzero ISM versus zero ISB does not affect convergence for a system of a fixed number of ODEs, we have illustrated that this makes the difference between stability and disastrous instability when applied to wave-type PDEs.

These results are immediately relevant to the non-stiff problems that arise for many important wave equations such as Maxwell's equations, acoustic (e.g., ultrasound) modeling, and elastic (e.g., seismic exploration) modeling. For nonlinear PDEs, linearized stability is normally required, and the present results are therefore again applicable.

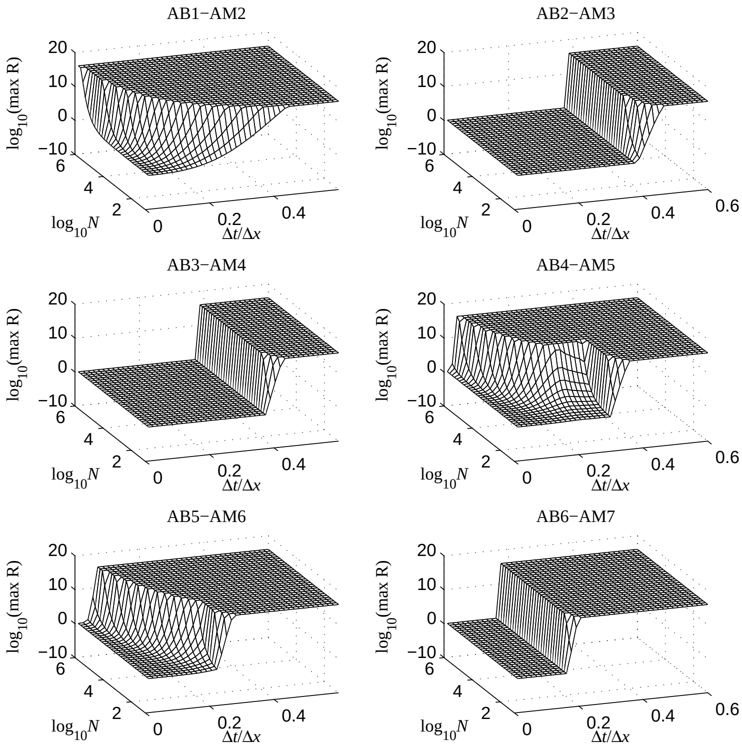

Fig. 5 Shown are the largest amplitude growth factors of any Fourier mode in the test problem (41) when advancing from $t = 0$ to $t = 10\pi$ using the first six AB($p-1$)-AMp methods, as a function of N (the number of nodes in the x-direction across $[-\pi, \pi]$) and the mesh aspect ratio $\frac{\Delta t}{\Delta x}$. The surfaces are truncated at the level $\max R = 10^{16}$.

Acknowledgements The authors are extremely grateful to Ernst Hairer for suggesting major simplifications in a previous form of this manuscript, in particular with regard to using the backward difference forms of AB and AM methods. We are also grateful for helpful comments from the referees that allowed us to improve our manuscript.

References

1. Atkinson, K.: An Introduction to Numerical Analysis. Wiley, New York (1989)
2. Fornberg, B.: A Practical Guide to Pseudospectral Methods. Cambridge University Press, Cambridge (1996)
3. Ghrist, M: High-order Finite Difference Methods for Wave Equations. Ph.D. thesis, Department of Applied Mathematics, University of Colorado-Boulder, Boulder, CO (2000)
4. Ghrist, M., Fornberg, B., Driscoll, T.A.: Staggered time integrators for wave equations, SIAM J. Num. Anal., *38*, 718–741 (2000)
5. Ghrist, M. and Fornberg, B.: Two results concerning the stability of staggered multistep methods, SIAM J. Num. Anal., *50*, 1849–1860 (2012)
6. Hairer, E., Nørsett, S.P., Wanner, G.: Solving Ordinary Differential Equations I, Springer-Verlag, Berlin (1991)

7. Hairer, E., Wanner, G.: Solving Ordinary Differential Equations II, 2nd edn., Springer-Verlag, Berlin (1996)
8. Henrici, P.: Discrete Variable Methods in Ordinary Differential Equations. John Wiley & Sons, New York (1962)
9. Iserles, A.: Numerical Analysis of Differential Equations. Cambridge University Press, Cambridge (1996)
10. Jeltsch, R.: A necessary condition for A-Stability of multistep multiderivative methods, Math. Comp., *30*, 739–746 (1976)